Understanding the solid-state assembly of pharmaceutically-relevant *N*,*N*-dimethyl-*O*-thiocarbamates in the absence of labile hydrogen bonds

Davin Tan,[a,*] Zi Xuan Ng,[a] Rakesh Ganguly,[a,b] Yongxin Li,[a] Han Sen Soo,[a] Felipe García[a,*]

a. Division of Chemistry and Biological Chemistry, School of Physical and Mathematical Sciences, Nanyang Technological University, 21 Nanyang Link, Singapore 637371, Singapore

b Chemistry Department, Shiv Nadar University, Gautam Buddha Nagar, India 201314

*E-mail: davin.tan@ntu.edu.sg, fgarcia@ntu.edu.sg

CCDC numbers: 1831294-1831307.

There are many pharmaceutical compounds that do not contain N-H, O-H, and S-H hydrogen-bond donor functional groups. Some of these compounds are *N*,*N*-disubstituted *O*-thiocarbamates which exhibit desirable medicinal properties, yet the study of these important molecules in the solid-state has been relatively unexplored. Herein, we report the synthesis and analysis of a series of *N*,*N*-dimethyl-O-thiocarbamates, and use X-ray diffraction techniques to gain insight into how these molecules self-assemble in the solid-state and discern certain packing patterns. It was observed that the aryl-thiocarbamate C-O bonds are twisted such that the planar aryl and carbamate moieties are orthogonal. Such a non-planar molecular geometry affects the way the molecules pack and crystal structure analyses revealed four general modes in which the molecules can associate in the solid-state, with some members of the series displaying isostructural relationships. The crystal structure of a well-known yet unreported *O*-thiocarbamate drug, Tolnaftate, is also reported. Additionally, Hirshfeld surface analysis was also performed on these compounds as well as several related *O*-thiocarbamates in the literature.

The ability to predict and dictate how molecules assemble in the solid-state has been the main cornerstone of crystal engineering.[1-5] Creating reproducible intermolecular interactions is thus crucial as it can be used as a design element to make different types of crystalline solids and materials, such as energetic compounds,[6-7] three-dimensional framework structures,[8-9] and cocrystals.[10-13] Formation of such supramolecular synthons[14-15] enables solid-state chemists to engineer how molecules assemble in the solid-state, and this is particularly essential in the context of pharmaceutical solids. Controlling how the active pharmaceutical ingredients (APIs) pack in the solid-state would affect their physicochemical

properties such as solubility, compressibility, and dissolution properties, which can in turn be fine-tuned.[16-19]

Most crystal engineering strategies, such as cocrystallization, typically depend on the construction of hydrogen bonding (HB) interactions using functional groups that contain labile or acidic protons such as amides, amines, alcohols, and carboxylic acids.[20-22] However, in many pharmaceutical molecules, such HB donor functional groups are not present, such as Diazepam, Midazolam, Progesterone, and Tamoxifen (**Figure 1**). In these cases, other types of intermolecular interactions may dominate and affect their assembly in the solid-state. These types of non-hydrogen bonding interactions include halogen bonds, π-π or CH-π interactions, and *van der Waals* forces.[23-25] One class of biologically active compounds that typically do not contain HB motifs is *O*-thiocarbamates. These compounds are pharmaceutically-relevant and are known to exhibit antibacterial and anti-fungal properties in marketed drugs such as Tolnaftate, Tolciclate, and Goitrin (**Figure 1**).[26-28]

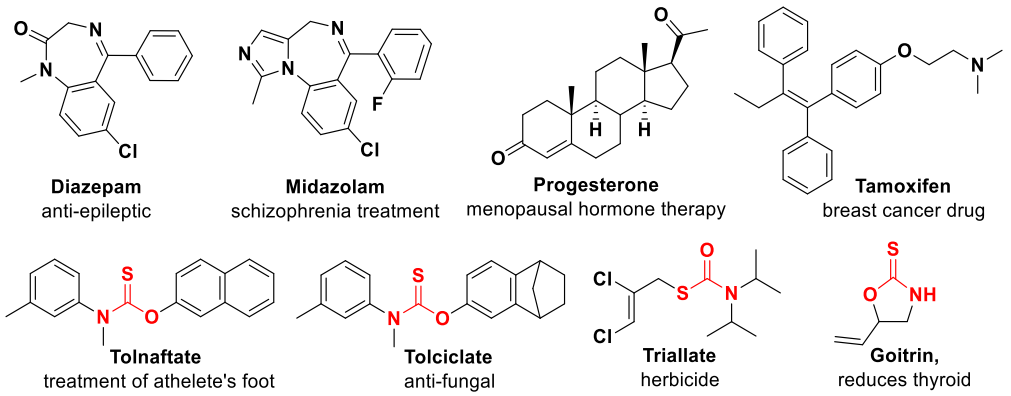

Figure 1. Examples of non-hydrogen bond donor drugs, including *O*-thiocarbamate containing pharmaceutical compounds.

However, a quick survey of the Cambridge Structural Database (CSD) revealed that approximately 290 metal-free organic compounds containing the *O*-thiocarbamate functional group have been reported.[29] This number dwindles to 91 for compounds that contain *N*,*N*-disubstituted *O*-thiocarbamates, in which the carbamate disubstituted N atoms act as HB donors. All these compounds containing *O*-thiocarbamate groups are isolated cases, except for a selected few examples. Specifically, Tiekink[30] and Kimber[31] have shown how unsubstituted *O*-thiocarbamates can be used as supramolecular synthons by forming dimeric pairs or linear chains held by N-H···S HB interactions. However, to the best of our knowledge, there has not been any study on understanding how *N*,*N*-disubstituted *O*-thiocarbamate molecules pack and assemble in the solid-state or what their intermolecular interactions are.

In addition, despite biological studies on the activity of Tolnaftate, a well-known drug for the treatment of athlete's foot,[26] its solid-state structure has not been reported yet. The lack of reports on the crystal structures of these pharmaceutically relevant compounds limits the understanding of how these molecules self-assemble in the solid-state in the absence of intermolecular HBs.

Hence, we set out to synthesize and characterize, using single-crystal X-ray diffraction (SCXRD), a series of related single-component *N*,*N*-dimethylaryl-*O*-thiocarbamates (**Figure 2**). These *O*-

thiocarbamates were carefully chosen whereby the substituents on the aryl rings contained a variety of functional groups, including electron withdrawing (**2**, **3**, **6**, **10**, **11**, **12**), electron donating (**4**, **5**, **9**), and sterically hindered groups *via* rational modification at the *ortho* position of the aryl ring (**7**, **8**), a polyaromatic system (**13**), as well as a *N*,*N*-diphenyl compound (**14**), and the commercial drug Tolnaftate (**15**).

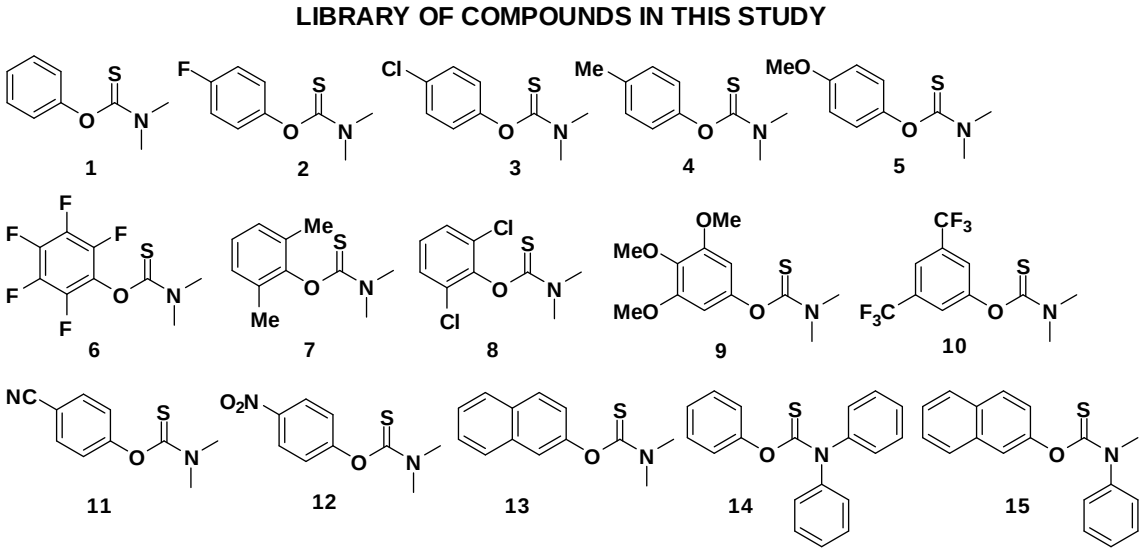

Figure 2. Various *N,N*-disubstituted *O*-thiocarbamates investigated.

From a structural standpoint, it may be assumed that thiocarbamates adopt a flat conformation. Such a flat molecular geometry is commonly seen in phenols, carbonates, amines, thioureas, or ureas,[32] where the aryl rings are coplanar with their respective functional group. However, based on the SCXRD data analysis, the molecular structure found in *O*-thiocarbamate species is far from being flat. Instead, the aryl-O bond is twisted such that the thiocarbamate moiety is almost perpendicular to the aryl ring. This orientation can be attributed to stereoelectronic factors since twisting of the aryl-O bond allows for delocalization and overlap between the two lone pairs of electrons on the O atom with the π electrons of the aromatic ring. Furthermore, the orthogonality between the thiocarbamate group and the aryl ring allows for the S atom to be oriented close to, and directly above, the *ipso* C atom of the aryl ring. This might explain the propensity of *O*-thiocarbamates to undergo isomerization, where the S and O atom exchange positions to form S-thiocarbamates under catalytic conditions or at elevated temperatures.[33-34]

The molecular structure of the studied *N*,*N*-dimethylaryl-*O*-thiocarbamates (*i.e.*, compounds **1**-**13**) can be described as two distinct planar groups that are perpendicular to each other, but are connected by an O atom (**Figure 3a**). One group (**Figure 3a**, in blue) represents the planar thiocarbamate moiety, while the other planar group (**Figure 3a**, in green) is the phenol moiety. The dihedral torsional angles and describe the twisting of the aryl C-O and the thiocarbamate C-O bonds, respectively. In the absence of directionally driven HBs, we hypothesized that these series of *N*,*N*-dimethylaryl-*O*-thiocarbamates would adopt similar packing motifs, since the overall geometrical shape, polarity, volume, and size of the compounds do not seem to differ significantly. Hence, it would be expected that the molecules should be primarily held together by weak van der Waals or π-π interactions in the solid-state.

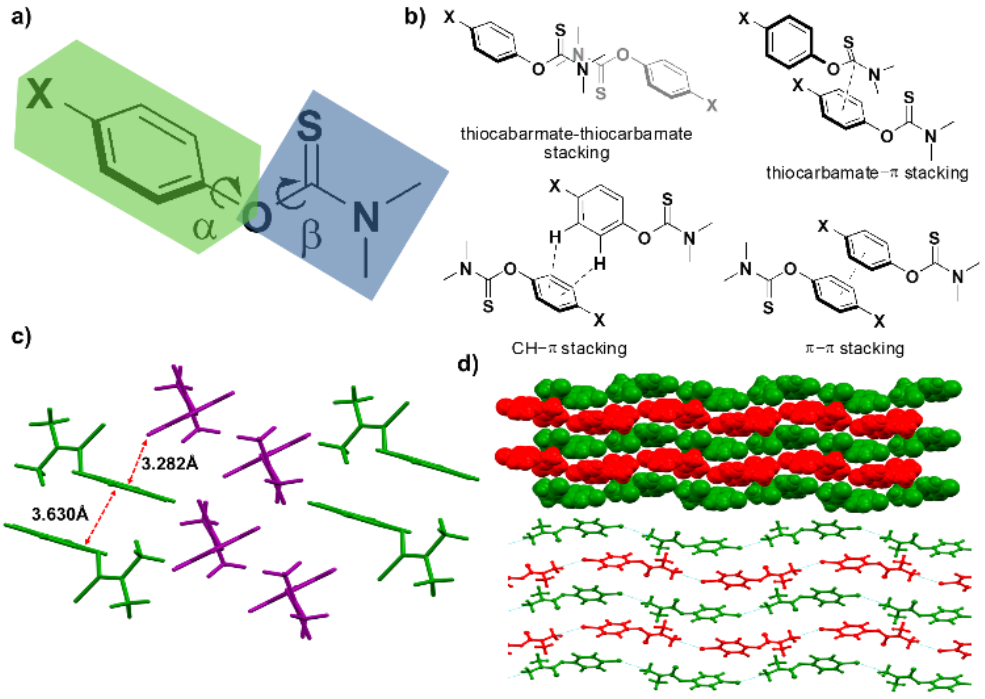

Figure 3. a) Generic structure of a *N*,*N*-dimethyl-*O*-thiocarbamate, illustrating the orthogonal thiocarbamate plane (in blue) and the substituted aryl plane (in green). b) The four intermolecular interactions observed from the library of compounds studies, namely thiocarbamate-thiocarbamate stacking in an *anti*- fashion, thiocarbamate-aryl stacking, CH-π stacking, and π-π stacking. c) Section of the crystal packing of **2**, denoting the C-H···π stacking between two layers and the π···π stacking within each layer. d) Space-filling and ball-and-stick representations of the isostructural molecular packing of **3** and **4** as viewed along the crystallographic *bc* plane. The two different layers are denoted in red and green.

Our initial attempts to grow diffraction quality crystals of **1** were not successful, yielding only oils or thin opaque films. Fortunately, SCXRD data were obtained for compounds **2**-**15**, and preliminary

analyses of their crystal structures revealed four distinct types of packing interactions, namely, *(i)* thiocarbamate-thiocarbamate stacking in an *anti*- fashion, *(ii)* thiocarbamate-aryl stacking, *(iii)* CH-π interaction, and *(iv)* π-π stacking (**Figure 3b**). Subsequently, more detailed analyses were conducted to discern any patterns between the molecular packing of the various compounds. Key interatomic distances and dihedral angles α and β are summarized in **Table S2.** Notably, the aryl C-O and *ipso* C-S bond distances, as well as the C-O-C and O-C-S angles did not show significant variation between the different compounds. However, there is a substantial difference in their dihedral angles, 73.72 – 119.26° and 0.18 – 22.91°, for α and β, respectively.

Compound **2** crystallizes in the triclinic *P*-1 space group and self-assembles forming alternating layers (**Figure 3c**). Each layer is held together by π-π stacking interactions, whereas different layers display CH-π interactions between them. Molecules of **3**, on the other hand, do not pack in the same manner as **2** despite having grown in the same solvent (*i.e.*, diethyl ether). Instead, **3** forms thiocarbamate-thiocarbamate and thiocarbamate-aryl stacking interactions producing relatively planar layers (**Figure 3d**), where alternating layers propagate in opposite directions.

According to Kitaigorodskii's *principle of close packing*, molecules with similar functional groups, shape, and size tend to adopt similar packing assemblies and are thus considered isostructural.[35] One good example of this is the chloro-methyl exchange rule,[36] whereby Cl and Me in related compounds can be isostructural and interchangeable within frameworks with similar crystal packing. Such isostructurality trends also persist within our sample group of *O*-thiocarbamate species. In particular, **3** and **4** obey the aforementioned chloro-methyl exchange rule. Both compounds crystallize in the same monoclinic $P2_1/c$ space group, have almost identical unit cell parameters, form similar thiocarbamate-thiocarbamate and thiocarbamate-aryl stacking interactions, and arrange in the same fashion (*i.e.*, they are isomorphous) (**Figure 3d**).[37]

In **5**, the presence of a methoxy group causes significant changes to the crystal structure. These methoxy substituents undergo weak intermolecular C-H···O HB interactions with adjacent methoxy groups, forming dimeric pairs. These pairs then form alternating interlocked grids (**Figure S31**) consisting of thiocarbamate-aryl interactions.

The crystal packing for **6** is also unique among our series of compounds. XRD analysis revealed that all the pentafluoroaryl rings within the crystal structure are facing the same direction, along the crystallographic *a*-axis (**Figure 4a**), while the thiocarbamate groups are all stacked facing the *b*-axis. When viewed along the *c*-axis (**Figure 4b**), it becomes clear that all the molecules assemble in the same manner and the thiocarbamate and aryl groups are almost perpendicular (α = 95.22°).

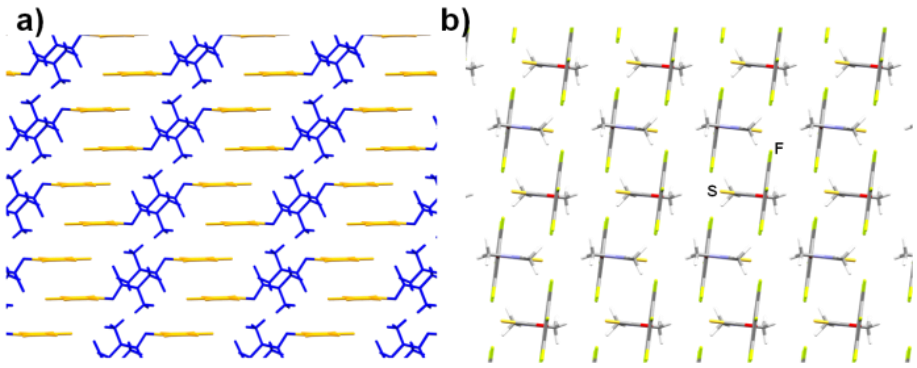

Figure 4. Capped sticks representation of the crystal structure of **6**, a) where the pentafluorophenyl group is highlighted in yellow and the thiocarbamate moiety is coloured in blue, as viewed along the *a*-axis (a) and along the *c*-axis (b).

The crystal structure for compound **7** has been previously reported (CCDC code **RAHLUK**).[38] Despite the isostructurality observed in **3** and **4**, the chloro-methyl exchange rule was not obeyed in **7** and **8**. The aryl rings of compound **7** form π-π and thiocarbamate-aryl interactions with one another. However, these interactions are slightly slip-stacked due to the presence of the Me groups at the 2' and 6' positions. These molecules then pack to form layers, in which molecules in alternating layers are rotated by 90 degrees (**Figure 5a**). Conversely, in **8**, the aryl groups only undergo π-π stacking interactions (inter-aryl stacking distance is about 3.384-3.696 Å). In addition, the thiocarbamate moieties are aligned in a head-to-tail fashion, forming anti-parallel catemers linked by weak intermolecular S···H_3CN interactions (**Figure 5b**).

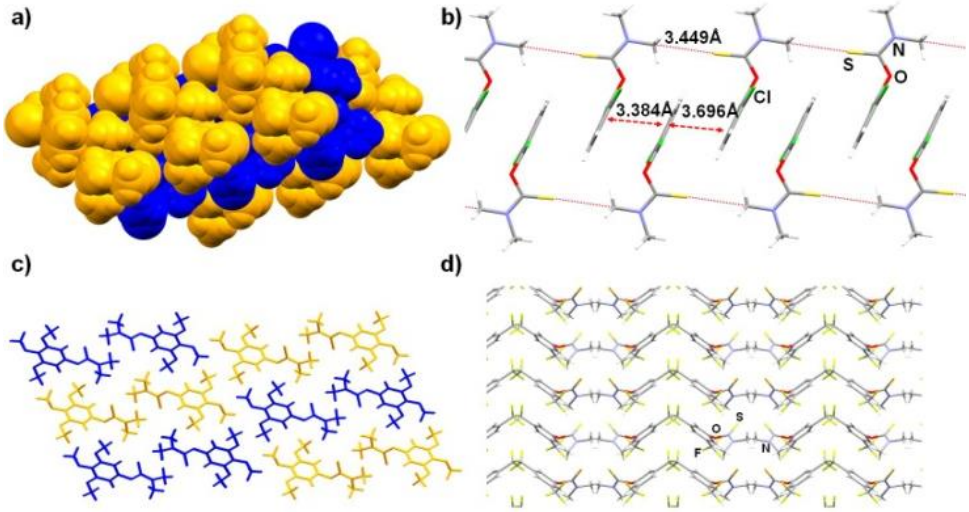

Figure 5. a) Space-filling representation of the crystal structure of **7**, denoting two distinct alternating layers in blue and orange. b) Capped sticks representation of **8**, illustrating π-π stacking interactions between the phenyl moieties. The thiocarbamate moieties of adjacent molecules are aligned into chains. c) Alternating dimeric molecules of **9** associated by thiocarbamate-thiocarbamate stacking are shown in yellow and blue. d) Fragment of the crystal structure of **10**, denoting the *zig-zag* wavy packing, propagating along the *b*-axis.

Similar to **5**, the molecules of **9** undergo weak intermolecular C-H···O HB interactions, forming an extensive network. However, unlike **5**, where the dimers are associated *via* tail-to-tail pairing of the methoxy groups. The molecules in **9** form dimeric pairs in which the planar thiocarbamate moieties are stacked, where alternating and adjacent pairs of molecules are rotated by 90° (**Figure 5c**).

Notably, molecular self-assembly for **10** does not seem to conform to any motif that was previously observed. Whereas the thiocarbamate and aryl moieties display weak intermolecular interactions in **2**-**9**, for **10**, neither the thiocarbamate nor the 3,5-bis(trifluoromethyl)aryl moieties are aligned or stacked parallel. Instead, the molecules of **10** form symmetrically associated pairs that are mirror-images. These pairs are arranged in a *zig-zag* manner forming parallel corrugated chains that propagate along the *b*-axis (**Figure 5d**). In addition, the S atom in the thiocarbamate functional group is also acting as a HB acceptor to the slightly acidic *ortho* C-H of the aryl ring (with a S···CF_3 distance of 3.736 Å).

In the solid-state structure of **11**, the molecules are arranged in a similar way as **6**, where the molecules form pairs in which the thiocarbamate moieties are slipped-stacked in an *anti*-fashion. These pairs of molecules assemble and form alternating layers that are opposite one another. However, unlike **6** where the aryl groups are parallel and face the same direction, allowing for π-π stacking between the layers, in **11**, the aryl groups are almost perpendicular. Colour coding (**Figure 6a**) the thiocarbamate and the 4-cyanoaryl moieties (in purple and cyan, respectively) shows how the perpendicular aryl groups display a linear corrugated arrangement along the crystallographic *a*-axis. In addition, the NCH_3 group of adjacent molecules are positioned directly above the slightly electron-deficient aryl rings, allowing for CH-π interactions to occur.

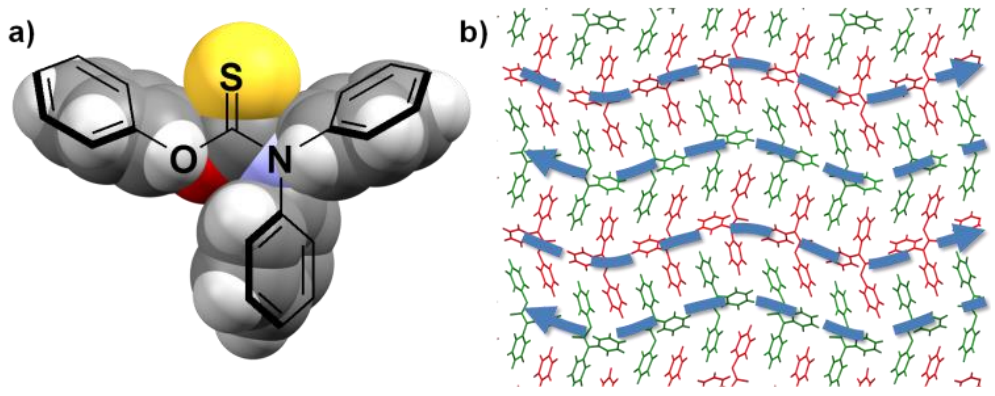

Figure 7. a) Space-filling representation of a Y-shaped molecule of **14**. b) Fragment of the crystal structure of **14**, showing alternating layers (in red and green) consisting of π-π stacking interactions. Blue arrows are drawn to depict the alternating layers propagating in opposite directions.

For **12**, the molecular packing motif is different from the rest of the compounds. In particular, the presence of highly polar NO_2 groups allows for weak CH···O interactions to form between the nitro group and NCH_3 groups of neighbouring molecules (**Figure S32**). The molecules are also arranged in ways where the aryl moieties are slipped-stacked (aryl-aryl distance *ca.* 3.428-3.503 Å) with alternating molecules rotated approximately 120°. These, in turn, form layers that propagate along the *a*-axis, with adjacent layers aligned in the opposite direction.

It was anticipated that the molecules of **13**, would self-assemble in similar fashion to compound **8**, where the thiocarbamates align head-to-tail forming catemeric chains with the naphthyl groups to create an extensive π-π stacked system. However, XRD analysis revealed that the molecules of **13** are, instead, aligned such that the thiocarbamate moieties of adjacent molecules are perpendicular. These, in turn, orientate their naphthyl rings above each other, allowing for an extensive network of CH-π interactions to be formed (**Figure 6b**).

In contrast to previous compounds where the *N*,*N*-dimethyl groups are small and coplanar to the thiocarbamate moiety, **14** comprises two bulky *N*,*N*-diphenyl rings. In this compound, the two bulky *N*,*N*-diphenyl rings are perpendicular to the thiocarbamate motif, giving rise to a Y-shaped molecule. In this case, the three bulky non-polar phenyl rings "shield" the more polar thiocarbamate functional group (**Figure 7a**). Without the presence of strong HB motifs or exposed polar functional groups, these molecules assemble and pack *via* the formation of weak π-π and CH-π interactions. The π-π interactions are only formed between the *O*-phenyl rings and not with the *N*-phenyl rings of adjacent molecules. Also, CH-π interactions are formed between the *O*-phenyl-to-*N*-phenyl and *N*-phenyl-to-*N*-phenyl rings. Unlike **8**, the π-π stacking interactions do not propagate extensively throughout crystal structure and are only observed between neighbouring pairs of molecules. Crystal packing analysis also revealed that the Y-shaped molecules of **14** form intercalated wave-like layers, in which alternating layers propagate in opposite directions (**Figure 7b**). Such a similar wave-like packing motif was also observed in **3**.

Lastly, X-ray diffraction quality crystals of **15** (*i.e.*, the anti-fungal drug Tolnaftate) were obtained after slow evaporation (three days) of the compound in an acetone and chloroform mixture. Despite having a similar Y-shaped geometry to **14**, molecules of **15** instead self-assembled to form inversely associated pairs that resemble the molecular packing of **13**, mainly consisting of π-π stacking interactions (aryl-aryl distance *ca.* 3.551 Å) between their naphthyl rings (**Figure 8**). Additionally, CH-π interactions (2.832-3.083 Å) between neighbouring *O*-naphthyl (in yellow) and between adjacent *N*-phenyl (in blue) rings of adjacent molecules can also be observed.

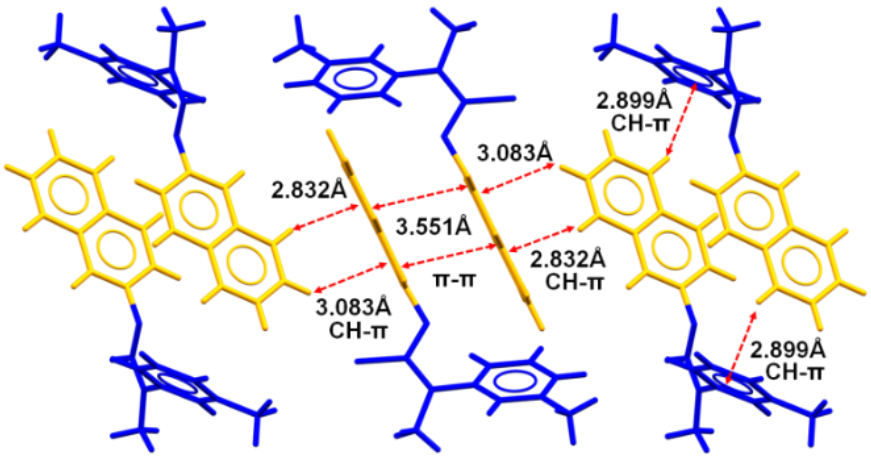

Figure 8. Capped stick representation of the crystal structure of Tolnaftate **15**, denoting π-π and CH-π interactions between adjacent naphthyl (in yellow) and phenyl (in blue) rings.

Finally, Hirshfeld surface analysis (**Figure S33-52**) were performed on all 14 crystal structures, as well as selected *O*-thiocarbamate compounds namely **ERIWEH**,[39] **GIQDES**,[40] **JELTUQ**,[41] **JELVAY**,[41] **VIVVUU**,[42] and **ZAHHUO**,[43] using CrystalExplorer.[44] For most of the compounds analysed, the largest percentage contribution to the interatomic contacts of the Hirshfeld surfaces were mainly C-H/H-C (~ 20-30%), H-H/H-H (~ 15-65%) and H-S/S-H (10-20%) short-range contacts. Representative noteworthy close contacts are highlighted in **Figure 7**, specifically for **14**, **15**, and **JELTUQ**. For instance, in compound **14**, H···H interactions appear as the largest regions of the fingerprint plots (51.7%) with a high concentration at $d_{external}$ (d_e) = $d_{internal}$ (d_i) ~ 1.4-1.6 Å.

Of particular interest, are the red coloured regions on the Hirshfeld surface, which indicate short-range contacts (highlighted by red arrows in **Figure 9**). These short-range interactions primarily correspond to C-H/H-C and H-H/H-H short contacts and can be attributed to intermolecular CH-π and van der Waals interactions. In some cases, such as **14** and **15**, these regions are observed near the S atom, which correspond to two sharp spikes on the fingerprint plot ($d_e + d_i$ ~ 2.0 Å) due to weak CH···S interactions from the thiocarbamate-aryl stacking (in **15**) or close proximity of the S atom with adjacent aryl CH or NCH_3 moieties (in **14**). Close contacts were also observed in **15** ($d_e + d_i$ ~ 1.9 Å), which are consistent with previously discussed aryl CH-π stacking from the naphthyl and phenyl moieties.

In compounds with several CH_3 groups on the phenyl and thiocarbamate moieties, such as **JELTUQ**, H···H interactions also contribute to the most significant percentage (65.4%) of the surface area with the highest concentration at $d_e = d_i$ ~ 1.4 Å. This is due to slipped-stacked thiocarbamate-aryl and thiocarbamate-thiocarbamate packing motifs. For compounds containing Cl or F substituents (*i.e.*, **2**,

3, **6**, **8**, **10**, and **GIQDES**) or strong HB acceptor moieties (*i.e.*, **5**, **9**, **11**, **12**, and **ERIWEH**, **VIVVUU**), other types of interactions dominate their Hirshfeld surfaces.

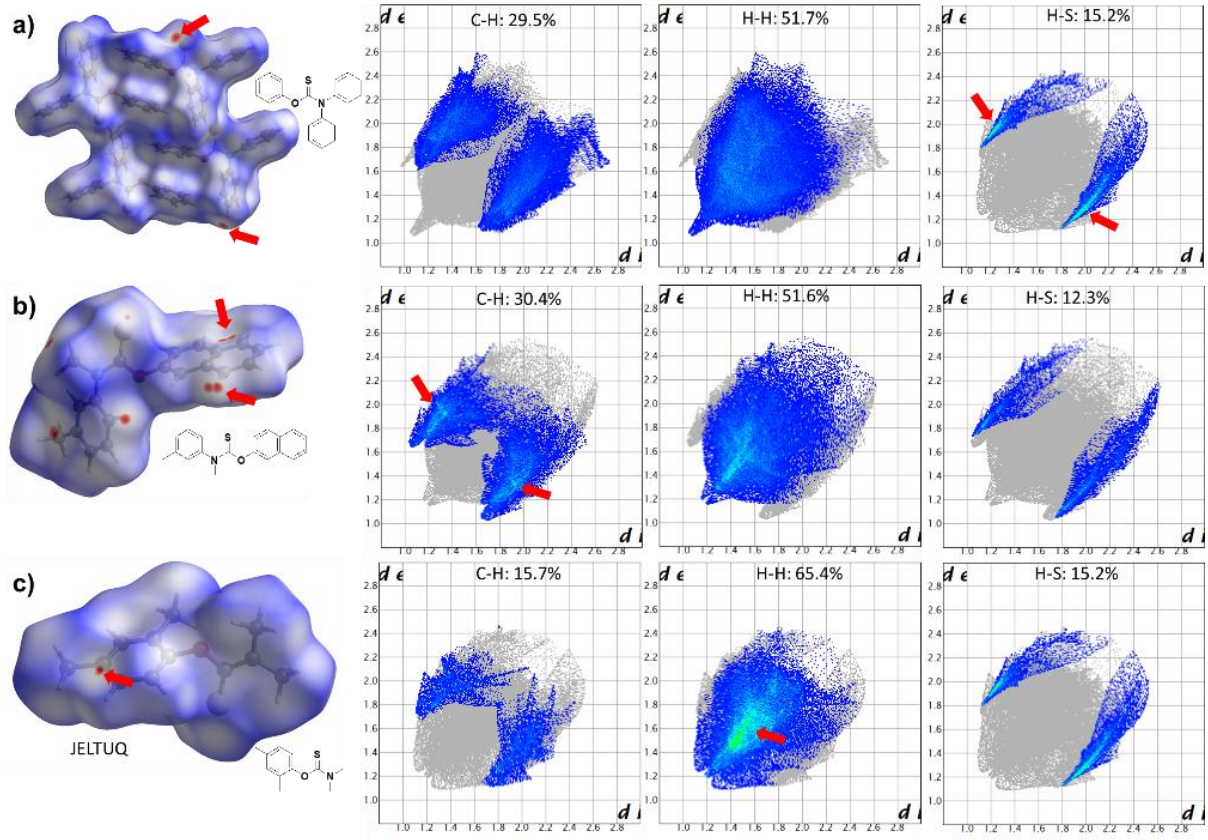

Figure 9. Hirshfeld surfaces mapped with d_{norm} (left) for (a) **14**, (b) **15**, and (c) JELTUQ, with their respective fingerprint plots showing the three largest percentage contributions of atoms (blue areas) within specific interacting pairs, namely C-H/H-C (left), H-H/H-H (middle), and H-S/S-H (right)

Conclusions

In summary, we have presented a library of *N*,*N*-disubstituted-*O*-thiocarbamates that do not contain labile protic functional groups and have analysed how these molecules self-assemble in the solid-state in the absence of HBs. Through these examples, we have identified four possible ways in which the molecules can stack and interact, and have observed similar packing patterns among the members, including isostructurality in the solid-state.

The presented study serves to demonstrate how minor alterations in the molecular structure, through substituents on the aryl ring, can have pronounced effects to the solid-state assembly. Using this library as a platform, good quality XRD data of the API Tolnaftate, whose solid-state structure was previously unknown, was obtained. Hirshfeld surface analysis was also performed on these compounds, including several selected *O*-thiocarbamates from the CSD database. We are currently exploring the cocrystallization of these thiocarbamates without the formation of HBs.

Acknowledgements

F.G. would like to thank A*STAR AME IRG (A1783c0003) and a NTU start-up grant (M4080552) for financial support. H.S.S. is grateful for the Singapore Ministry of Education Academic Research Fund Tier 1 grants RG 111/18 and RT 05/19. H.S.S. also acknowledges that this project is supported by A*STAR under the AME IRG grants A1783c0003, A1783c0002, and A1783c0007. D.T. would like to thank A*STAR for a postdoctoral research fellowship.

Notes and references

1. G. R. Desiraju, *J. Am. Chem. Soc.* 2013, **135**, 9952-9967.

2. B. Moulton and M. J. Zaworotko, *Chem. Rev.* 2001, **101**, 1629-1658.

3. A. Nangia, *J. Chem. Sci.* 2010, **122**, 295-310.

4. C. B. Aakeröy, N. R. Champness and C. Janiak, *CrystEngComm*, 2010, **12**, 22-43.

5. K. Biradha, C.-Y. Su and J. J. Vittal, *Cryst. Growth Des.* 2011, **11**, 875-886.

6. C. B. Aakeröy, T. K. Wijethunga and J. Desper, *Chem. Eur. J.* 2015, **21**, 11029-11037.

7. O. Bolton and A. J. Matzger, *Angew. Chem. Int. Ed.* 2011, **50**, 8960-8963.

8. W. Yang, A. Greenaway, X. Lin, R. Matsuda, A. J. Blake, C. Wilson, W. Lewis, P. Hubberstey, S. Kitagawa, N. R. Champness and M. Schröder, *J. Am. Chem. Soc.* 2010, **132**, 14457-14469.

9. T. Adachi and M. D. Ward, *Acc. Chem. Res.* 2016*,* **49**, 2669-2679.

10. S. Cherukuvada and T. N. G. Row, *Cryst. Growth Des.* 2014, **14**, 4187-4198.

11. F. Topić and K. Rissanen, *J. Am. Chem. Soc.*, 2016, **138**, 6610-6616.

12. D. Braga, L. Maini, F. Grepioni, A. De Cian, O. Félix, J. Fischer and M. W. Hosseini, *New J. Chem.* 2000, **24**, 547-553.

13. M. K. Corpinot, S. A. Stratford, M. Arhangelskis, J. Anka-Lufford, I. Halasz, N. Judaš, W. Jones and D.-K. Bučar, *CrystEngComm*, 2016, **18**, 5434-5439.

14. G. R. Desiraju, *Angew. Chem. Int Ed.* **1995**, *31,* 2311-2321.

15. J. W. Steed and J. L. Atwood, *Supramolecular Chemistry 2nd ed.*, 2009, John Wiley & Sons, Ltd., United Kingdom.

16. O. V. Shishkin, R. I. Zubatyuk, S. V. Shishkina, V. V. Dyakonenkoa and V. V. Medviediev, *Phys. Chem. Chem. Phys.*, 2014, **16**, 6773-6786.

17. N. Blagden, M. de Matas, P. T. Gavan and P. York, *Adv. Drug Delivery Rev.* 2007, **59**, 617-630.

18. S. Karki, T. Friščić, L. Fábián P. R. Laity, G. M. Day and W. Jones, *Adv. Mater.* 2009, **21**, 3905-3909.

19. D. J. Good and N. Rodríguez-Hornedo, *Cryst. Growth Des.* 2009, **9**, 2252-2264.

20. A. N. Sokolov, T. Friščić and L. R. MacGillivray, *J. Am. Chem. Soc.*, 2006, **128**, 2806-2807.

21. H. Wang, G. Gurau, J. Shamshina, O. A. Cojocaru, J. Janikowski, D. R. MacFarlane, J. H. Davis Jr. and R. D. Rogers, *Chem. Sci.*, 2014, **5**, 3449-3456.

22. D. P. Ericson, Z. P. Zurfluh-Cunningham, R. H. Groeneman, E. Elacqua, E. W. Reinheimer, B. C. Noll and L. R. MacGillivray *Cryst. Growth Des.* 2015, **15**, 5744-5748.

23. G. Cavallo, P. Metrangolo, R. Milani, T. Pilati, A. Priimagi, G. Resnati, G. Terraneo, *Chem. Rev.*, 2016, **116**, 2478-2601.

24. S. J. Dalgarno, P. K. Thallapally, L. J. Barbour and J. L. Atwood, *Chem. Soc. Rev.*, 2007, **36**, 236-245.

25. K. J. Ardila-Fierro, Va. André, D. Tan, M. T. Duarte, R. W. Lancaster, P. G. Karamertzanis and T. Friščić, *Cryst. Growth Des.* 2015, **15**, 1492-1501.

26. N. S. Ryder, I. Frank and M.-C. Dupont, *Antimicrob. Agents Chemother.*, 1986, **29**, 858-860.

27. A. Bianchi, G. Monti and I. de Carner, *Antimicrob. Agents Chemother.*, 1977, **12**, 429-430.

28. C. Faiman, R. J. Ryan and H. J. Eichel, *Endocrinology*, 1967, **81**, 88-92.

29. Derived from reported structures in the Cambridge Structural Database (CSD), CCDC SEARCH date 10 June 2020.

30. F. S. Kuan, F. Mohr, P. P. Tadbuppa and Edward R. T. Tiekink, *CrystEngComm*, 2007, **9**, 574–581.

31. N. H. Slater, B. R. Buckley, M. R. J. Elsegood, S. J. Teat and M. C. Kimber, *Cryst. Growth Des.* 2016, **16**, 3846-3852.

32. R. Custelcean, *Chem. Commun.*, 2008, 295-307.

33. A. J. Perkowski, C. L. Cruz and D. A. Nicewicz, *J. Am. Chem. Soc.* 2015, **50**, 15684-15687.

34. T. A. Ablott, M. Turzer, S. G. Telfer and C. Richardson, *Cryst. Growth Des.* 2016, **16**, 7067−7073.

35. A. I. Kitaigorodskii, *Acta Cryst.*, 1965, **18**, 585-590.

36. G. R. Desiraju and J. A. R. P. Sarma, *J. Chem. Sci.* 1986, **96**, 599-605.

37. N. K. Nath and A. Nangia, *Cryst. Growth Des.*, 2012, **12**, 5411-5425.

38. M. Yamada CCDC 1422039, *Experimental Crystal Structure Determination*, **2017**, *DOI: 10.5517/ccdc.csd.cc1jqr77*.

39. C. M. L. Vande Velde, H. J. Geise, F. Blockhuys, *Acta Cryst.*, 2004, **E60**, o199-o200.

40. K. Eriksen, A. Ulfkjær, T. I. Sølling, M. Pittelkow, *J. Org. Chem.,* 2018, **83**, 10786–10797.

41. A. Flores-Figueroa, V. Arista-M., D. Talancón-Sánchez, I. Castillo, *J. Braz. Chem. Soc.*, 16, **397-403**, 2005.

42. D. Shi, S. Chen, B. Dong, Y. Zhang, C. Sheng, T. D. James, Y. Guo, *Chem. Sci.*, 2019, **10**, 3715-3722.

R. Zhang, L. Xu, H. Chen, Z. Qin, Y. Zhao, Z. Ni, *Chem. Res. Chin. Univ.,* 2015, **31**, 224–227.

M. J. Turner, J. J. McKinnon, S. K. Wolff, D. J. Grimwood, P. R. Spackman, D. Jayatilaka, M. A. Spackman, CrystalExplorer17, **2017**, University of Western Australia, *https://hirshfeldsurface.net*.